Extensional Waves in a Sandwich Plate With Interface Slip

Article *in* Journal of vibration and acoustics · February 2015

DOI: 10.1115/1.4029334

Feng Jin

Xi'an Jiaotong University

W. Q. Chen

Zhejiang University

Peng Li
School of Human Settlements and Civil Engineering,
Xi'an Jiaotong University,
Xi'an, Shaanxi 710049, China

Feng Jin[1]
State Key Laboratory for Strength and Vibration of Mechanical Structures,
Xi'an Jiaotong University,
Xi'an, Shaanxi 710049, China
e-mail: jinfengzhao@263.net

Weiqiu Chen
Department of Engineering Mechanics,
Zhejiang University,
Hangzhou, Zhejiang 310027, China

Jiashi Yang
Department of Mechanical and Materials Engineering,
University of Nebraska-Lincoln,
Lincoln, NE 68588

Extensional Waves in a Sandwich Plate With Interface Slip

The two-dimensional (2D) equations for thin elastic plates are used to study extensional motions of a sandwich plate with weak interfaces. The interfaces are governed by the shear-slip model that possesses interface elasticity and allows for a discontinuity of the tangential displacements at the interfaces. Equations for the individual layers of the sandwich plate are coupled by the interface conditions. Through a procedure initiated by Mindlin, the layer equations can be written into equations for the collective motion of the layers representing the extensional motion of the sandwich plate, and equations for the relative motions of the layers with respect to each other representing the symmetric thickness-shear motion of the sandwich plate. The use of plate equations results in relatively simpler models compared to the equations of three-dimensional (3D) elasticity. Solutions to a few useful problems are presented. These include the propagation of straight-crested waves in an unbounded plate with weak interfaces, the reflection of extensional waves at the joint between a perfectly bonded sandwich plate and a sandwich plate with weak interfaces, and the vibration of a finite sandwich plate with weak interfaces. [DOI: 10.1115/1.4029334]

Keywords: imperfect interface, shear-slip model, straight-crested waves, dispersion curves, reflection coefficient

1 Introduction

Multilayered plates with interfaces among layers of different materials are common structures in many engineering fields. Many issues have been addressed about interface, including its simulation in mixed concrete-steel beams [1], predicting of thermal conductivity in composite materials [2], macroscopic analysis of elasticity [3], micromechanical explanation [4], and so forth. Very often a gluing substance, e.g., epoxy, is applied to the interfaces. In other cases, the molecules of neighboring materials interpenetrate into each other to form a bonding layer. In the simplest mechanics description, an interface is treated as a geometric surface where perfect bonding with continuous displacement and traction is assumed. More realistically, an interface may be viewed as a thin layer whose material properties are different from those of the bulk materials meeting at the interface. Interfaces at which some or all of the mechanical continuity conditions are relaxed are called weak, nonrigidly bonded, or imperfectly bonded interfaces. Researchers have developed imperfect interface models with different levels of sophistication. Mechanical properties and behaviors of weak interfaces described by different models have been studied both experimentally [5–8] and theoretically [9–12]. Specifically, for dynamic problems relevant to the present paper, wave propagation in unbounded domains [13–23] and thickness vibrations of plates [24–27] have been analyzed for various applications including material characterization, structural strength consideration, acoustic wave sensors, and nondestructive evaluation. Static and dynamic problems of composite beams with weak interfaces were studied in Refs. [28–30]. More references can be found in a review article [31].

Different from most of the previous analyses of plates with weak interfaces, instead of using the exact 3D equations of elasticity or piezoelectricity, we use the approximate 2D equations of elastic plates to study the extensional motion of an elastic sandwich plate symmetric about its middle plane with two weak interfaces. The specific way that we employ the 2D equations follows a unique procedure developed by Mindlin [32]. It differs from the 2D approach by other researchers [9,33] in that Mindlin's procedure is based on 2D equations of individual layers. This procedure involves combining 2D equations for individual layers through interface continuity conditions. As a result, in addition to the 2D equations for the motions of the layered plate as a whole, this procedure also leads to 2D equations for the motions of the individual layers which can be used to calculate the interface stress distributions conveniently. Mindlin's procedure was initially used for layered elastic plates [32] with perfectly bonded interfaces and was later extended to layered elastic plates with intrinsic stresses [34] and layered multiphysical plates [35–37] with perfect interfaces.

In this paper, we generalize Mindlin's procedure from layered plates with perfect interfaces to layered plates with weak interfaces. The weak interfaces in our sandwich plate are governed by the widely used shear-slip model [9,10]. In this model, an interface has its own elasticity but not inertia. The traction is still continuous across the interface but the tangential displacements are allowed to have a jump discontinuity. In Sec. 2, the equations and interface conditions are presented. Sections 3–5 show solutions to a few basic and useful problems including the propagation of straight-crested waves, wave reflection and transmission at the joint between a perfectly bonded sandwich plate and a sandwich plate with weak interfaces, and vibration of a finite sandwich plate with weak interfaces. A few interesting and useful results are obtained and discussed.

2 2D Equations for a Sandwich Plate With Weak Interfaces

Consider the thin sandwich plate in Fig. 1. x_1 and x_3 are in the middle plane. x_2 is along the plate normal. For convenience, we call the middle layer the core, and the top and bottom layers films.

[1]Corresponding author.

Contributed by the Technical Committee on Vibration and Sound of ASME for publication in the JOURNAL OF VIBRATION AND ACOUSTICS. Manuscript received December 18, 2012; final manuscript received December 5, 2014; published online January 27, 2015. Assoc. Editor: Walter Lacarbonara.

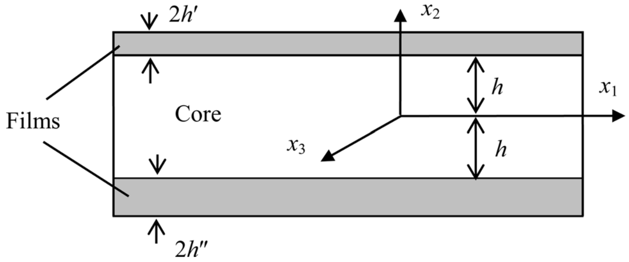

Fig. 1 A sandwich plate with weak interfaces

At this point, the two films may be different, with the parameters of the top film indicated by a prime and those of the bottom film by a double prime. Later, the two films will be made identical so that the sandwich plate is symmetric about its middle plane to ensure the existence of extensional motions symmetric about the middle plane without bending. The 2D Cartesian tensor notation is employed, with the summation convention for repeated indices. A comma followed by an index denotes a partial derivative with respect to the coordinate associated with the index. a, b, c, d range over the in-plane indices of 1 and 3 but skip 2.

Consider the core of thickness $2h$ first. For extensional motions, the in-plane components of the displacement vector are approximated by

$$u_a \cong u_a(x_b, t), \quad a, b = 1, 3 \tag{1}$$

The in-plane extensional and shear strain components are

$$S_{ab} = \frac{1}{2}(u_{a,b} + u_{b,a}) \tag{2}$$

The in-plane stress resultants N_{ab} are obtained by integrating the corresponding stress components T_{ab} through the plate thickness

$$N_{ab} \equiv \int_{-h}^{h} T_{ab} dx_2 = 2h\gamma_{abcd} S_{cd} = 2h\gamma_{abcd} u_{c,d} \tag{3}$$

where we have inserted the 2D or plane-stress constitutive relations [32,38]. γ_{abcd} are the 2D elastic constants for thin plates [32,38]. They are obtained from the 3D elastic constants by the stress relaxation condition $T_{21} = T_{22} = T_{23} = 0$. The 2D stress equations of motion are obtained by integrating the two in-plane ones of the 3D equations of motion through the plate thickness, with the following result:

$$N_{ab,a} + T_{2b}|_h - T_{2b}|_{-h} = 2h\rho\ddot{u}_b \tag{4}$$

where $T_{2b}|_h$ and $T_{2b}|_{-h}$ are the shear stresses at the top and bottom surfaces of the core, or the interface shear stresses of the sandwich plate. Substituting Eq. (3) into Eq. (4), we obtain the displacement equation of motion for the core

$$2h\gamma_{abcd} u_{c,da} + T_{2b}|_h - T_{2b}|_{-h} = 2h\rho\ddot{u}_b \tag{5}$$

Fields associated with the upper and lower films are also designated by primes and double primes, respectively. Then, corresponding to Eqs. (2)–(5), the equations for the extensional motion of the upper film are

$$S'_{ab} = \frac{1}{2}(u'_{a,b} + u'_{b,a}) \tag{6}$$

$$N'_{ab} = 2h'\gamma'_{abcd} S'_{cd} = 2h'\gamma'_{abcd} u'_{c,d} \tag{7}$$

$$N'_{ab,a} + T'_{2b}|_{h'} - T'_{2b}|_{-h'} = 2h'\rho'\ddot{u}'_b \tag{8}$$

$$2h'\gamma'_{abcd} u'_{c,da} + T'_{2b}|_{h'} - T'_{2b}|_{-h'} = 2h'\rho'\ddot{u}'_b \tag{9}$$

Similarly, for the lower film, we have

$$S''_{ab} = \frac{1}{2}(u''_{a,b} + u''_{b,a}) \tag{10}$$

$$N''_{ab} = 2h''\gamma''_{abcd} S''_{cd} = 2h''\gamma''_{abcd} u''_{c,d} \tag{11}$$

$$N''_{ab,a} + T''_{2b}|_{h''} - T''_{2b}|_{-h''} = 2h''\rho''\ddot{u}''_b \tag{12}$$

$$2h''\gamma''_{abcd} u''_{c,da} + T''_{2b}|_{h''} - T''_{2b}|_{-h''} = 2h''\rho''\ddot{u}''_b \tag{13}$$

According to the shear-slip interface model [9,10], the interface shear stresses are related to the relative interface shear displacements of the core and the films through

$$\begin{aligned} T'_{2b}|_{-h'} &= T_{2b}|_h = K'(u'_b - u_b) \\ T''_{2b}|_{h''} &= T_{2b}|_{-h} = K''(u_b - u''_b) \end{aligned} \tag{14}$$

where K' and K'' are the interface shear elastic constants. We note that in the more general case of anisotropic interfaces K' and K'' should be two-by-two matrices. Substitution of Eq. (14) into Eqs. (5), (9), and (13) gives

$$2h\gamma_{abcd} u_{c,da} + K'(u'_b - u_b) - K''(u_b - u''_b) = 2h\rho\ddot{u}_b \tag{15}$$

$$2h'\gamma'_{abcd} u'_{c,da} + T'_{2b}|_{h'} - K'(u'_b - u_b) = 2h'\rho'\ddot{u}'_b \tag{16}$$

$$2h''\gamma''_{abcd} u''_{c,da} + K''(u_b - u''_b) - T''_{2b}|_{-h''} = 2h''\rho''\ddot{u}''_b \tag{17}$$

Equations (15)–(17) form a complete set of equations for the extensional motions of the sandwich plate including the effects of the weak interfaces. They are three vector equations for u_b, u'_b, and u''_b. Since each layer has its own displacement vector, edge conditions may be specified individually for each layer.

Equations (15)–(17) can be manipulated to produce mathematically more convenient or physically more revealing equations. For example, if we add Eqs. (15)–(17) together, we obtain

$$\mathcal{N}_{ab,a} + T'_{2b}|_{h'} - T''_{2b}|_{-h''} = 2h\rho\ddot{u}_b + 2h'\rho'\ddot{u}'_b + 2h''\rho''\ddot{u}''_b \tag{18}$$

where we have denoted

$$\begin{aligned} \mathcal{N}_{ab} &= N_{ab} + N'_{ab} + N''_{ab} \\ &= 2h\gamma_{abcd} u_{c,d} + 2h'\gamma'_{abcd} u'_{c,d} + 2h''\gamma''_{abcd} u''_{c,d} \end{aligned} \tag{19}$$

$\mathcal{N}_{ab}$ represent the total extensional resultants over the cross section of the sandwich plate. Equation (18) describes the motion of the sandwich plate as a whole. It is convenient to use because it does not have the interface stresses explicitly. However, Eq. (18) alone does not represent a complete description of the sandwich plate when there are weak interfaces. In the special case of perfect bonding with $u'_b = u''_b = u_b$, Eq. (18) reduces to the conventional or classical extensional equation of a sandwich plate with perfectly bonded interfaces.

We now specialize the above equations to the case of identical films in symmetric motions with $u''_b = u'_b$. In this case, only one of Eqs. (16) and (17) is needed. For example, Eqs. (15) and (16) together form a complete description.

$$2h\gamma_{abcd} u_{c,da} + 2K'(u'_b - u_b) = 2h\rho\ddot{u}_b \tag{20}$$

$$2h'\gamma'_{abcd} u'_{c,da} - K'(u'_b - u_b) = 2h'\rho'\ddot{u}'_b \tag{21}$$

where we have dropped the surface load $T'_{2b}|_{h'}$ in Eq. (16) because they will not be needed in the problems to be analyzed below.

Equations (20) and (21) can be written into other forms for different purposes. For example, from Eq. (20), we can write u'_b in terms of u_b

$$K'u'_b = h\rho\ddot{u}_b + K'u_b - h\gamma_{abcd}u_{c,da} \quad (22)$$

or, from Eq. (21), u_b in terms of u'_b

$$K'u_b = 2h'\rho'\ddot{u}'_b + K'u'_b - 2h'\gamma'_{abcd}u'_{c,da} \quad (23)$$

We can also add Eqs. (20) and (21) to obtain a single equation for the motion of the sandwich plate as a whole

$$h\gamma_{abcd}u_{c,da} + 2h'\gamma'_{abcd}u'_{c,da} = h\rho\ddot{u}_b + 2h'\rho'\ddot{u}'_b \quad (24)$$

Equation (24) with either Eqs. (20) or (21) also gives a complete description of the sandwich plate.

3 Wave Propagation in an Unbounded Plate

As the first example for the application of the equations in Sec. 2, we consider the propagation of straight-crested waves in the x_1 direction of an unbounded plate, i.e., $u_1 = u_1(x_1, t)$, $u'_1 = u'_1(x_1, t)$, and $u_3 = u'_3 = 0$. In this case, Eqs. (24) and (21) take the following form:

$$\begin{aligned} h\gamma u_{1,11} + 2h'\gamma' u'_{1,11} &= h\rho\ddot{u}_1 + 2h'\rho'\ddot{u}'_1 \\ K'u'_1 &= h\rho\ddot{u}_1 + K'u_1 - h\gamma u_{1,11} \end{aligned} \quad (25)$$

where

$$\gamma = \gamma_{1111}, \quad \gamma' = \gamma'_{1111} \quad (26)$$

We note that the film displacement u'_1 can be eliminated by substituting Eq. $(25)_2$ into Eq. $(25)_1$, resulting in a fourth-order equation for u_1

$$\begin{aligned} &(h\gamma + 2h'\gamma')u_{1,11} - (h\rho + 2h'\rho')\ddot{u}_1 \\ &= 2h'\rho'\left(\frac{h\rho\ddot{\ddot{u}}_1 - h\gamma\ddot{u}_{1,11}}{K'}\right) - 2h'\gamma'\left(\frac{h\rho\ddot{u}_1 - h\gamma u_{1,11}}{K'}\right)_{,11} \end{aligned} \quad (27)$$

Equation (27) differs from the conventional equation for the extension of a sandwich plate with perfect bonding by the two terms on the right-hand side. They are associated with various fourth-order derivatives and indicate dispersive waves. This is fundamentally different from the classical extensional waves. We note that the two terms on the right-hand side of Eq. (27) disappear when $K' \to \infty$. We look for a propagating wave solution of Eq. (25) by letting

$$u_1 = C \exp i(\omega t - \xi x_1), \quad u'_1 = C' \exp i(\omega t - \xi x_1) \quad (28)$$

where C, C', ω, and ξ are undetermined constants. Substitution of Eq. (28) into Eq. (25) yields two linear homogeneous equations for C and C'

$$\begin{aligned} (h\rho\omega^2 - h\gamma\xi^2)C + (2h'\rho'\omega^2 - 2h'\gamma'\xi^2)C' &= 0 \\ (h\rho\omega^2 - h\gamma\xi^2 - K')C + K'C' &= 0 \end{aligned} \quad (29)$$

For nontrivial solutions, the determinant of the coefficient matrix of Eq. (29) has to vanish, i.e.,

$$\begin{aligned} &(h\rho + 2h'\rho')\omega^2 - (h\gamma + 2h'\gamma')\xi^2 \\ &- \frac{1}{K}\left[(h\rho\omega^2 - h\gamma\xi^2)(2h'\rho'\omega^2 - 2h'\gamma'\xi^2)\right] = 0 \end{aligned} \quad (30)$$

which determines the dispersion relations of the waves described by Eq. (28). Let

$$\begin{aligned} &\alpha = \frac{2h'}{h}, \quad \beta = \frac{\rho'}{\rho}, \quad c = \sqrt{\frac{\gamma}{\rho}}, \quad c' = \sqrt{\frac{\gamma'}{\rho'}} \\ &\Omega = \frac{h\omega}{c}, \quad X = \xi h, \quad \Gamma = \frac{\gamma}{K'h} \end{aligned} \quad (31)$$

Then Eq. (30) can be written into the following dimensionless form:

$$(1+\alpha\beta)\Omega^2 - \left(1+\alpha\beta\frac{c'^2}{c^2}\right)X^2 - \Gamma\alpha\beta(\Omega^2 - X^2)\left(\Omega^2 - \frac{c'^2}{c^2}X^2\right) = 0 \quad (32)$$

In terms of $\xi^2(\omega)$ (or $\omega^2(\xi)$), Eq. (32) determines two branches of dispersion relations denoted by $\xi^{(1)}(\omega)$ and $\xi^{(2)}(\omega)$. When $\xi = 0$ or $X = 0$, Eq. (32) reduces to

$$(1+\alpha\beta)\Omega^2 - \Gamma\alpha\beta\Omega^4 = 0 \quad (33)$$

Equation (33) has two roots

$$\begin{aligned} &\Omega_1 = 0, \quad \Omega_2 = \sqrt{\frac{1+\alpha\beta}{\Gamma\alpha\beta}} \quad \text{or} \quad \omega_1 = 0, \\ &\omega_2 = \sqrt{K'\left(\frac{1}{h\rho} + \frac{1}{2h'\rho'}\right)} \end{aligned} \quad (34)$$

For perfect interface bonding, $\omega_2 = \infty$.

We plot the two dispersion relations for real and pure imaginary wave numbers in Fig. 2. For the case of perfect interface bonding with $\Gamma = 0$, there is only one branch going through the origin for the classical extensional wave. When weak interfaces are present and $\Gamma > 0$, there are two branches. One is close to the classical extensional wave. The other has a finite intercept with the frequency axis. These intercepts are called cutoff frequencies below which the wave number becomes pure imaginary and the corresponding waves cannot propagate. This branch corresponds to the so-called symmetric thickness-shear wave in an elastic plate [38]. The appearance of this second wave when there are weak interfaces is qualitatively different from a classical sandwich plate with perfect interfaces. When K' decreases or Γ increases, the interface bonding becomes weaker and the frequencies of the waves become lower as expected.

Up to now, we have adopted the approximate 2D equations of elastic plates, which first developed by Mindlin, to study the extensional motion of an elastic sandwich plate symmetric about its middle plane with two weak interfaces. This method is totally different from most of the previous analyses described in the Introduction. An additional mode that is caused by imperfect

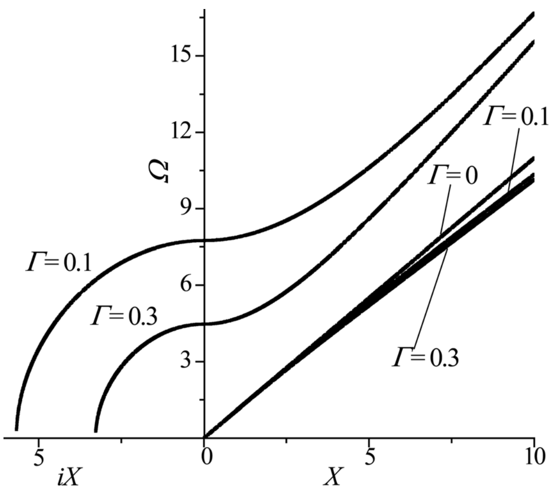

Fig. 2 Dispersion curves determined by Eq. (32)

interface has been found using this method. In fact, the similar phenomenon has been revealed recently in our publication [39] by using of perturbation method, which can correct our results to some extent. Maybe some other numerical integration methods can be used to solve this problem, which will be explored in the near future.

Corresponding to the two branches of dispersion relations, there are two amplitude ratios determined by one of Eq. (29), e.g., Eq. $(29)_1$

$$\beta^{(1)} = \frac{C'}{C} = -\frac{h\rho\omega^2 - h\gamma(\xi^{(1)})^2 - K'}{K'}$$
$$\beta^{(2)} = \frac{C'}{C} = -\frac{h\rho\omega^2 - h\gamma(\xi^{(2)})^2 - K'}{K'} \tag{35}$$

Then the general solution to Eq. (25) in the form of Eq. (28) can be written as

$$\left\{\begin{matrix} u_1 \\ u_1' \end{matrix}\right\} = C^{(1)}\left\{\begin{matrix} 1 \\ \beta^{(1)} \end{matrix}\right\}\exp i\left(\omega t - \xi^{(1)}x_1\right) + C^{(2)}\left\{\begin{matrix} 1 \\ \beta^{(2)} \end{matrix}\right\}\exp i\left(\omega t - \xi^{(2)}x_1\right) \tag{36}$$

where $C^{(1)}$ and $C^{(2)}$ are arbitrary constants. This will be useful in Sec. 4.

4 Reflection and Transmission at a Joint

Next, we consider two semi-infinite sandwich plates joined together (see Fig. 3). The left half is perfectly bonded. The right half has weak interfaces. We send an extensional wave from the left end. When it reaches the joint, it feels the beginning of the weak interfaces and gets reflected and transmitted. This is a basic problem for nondestructive evaluation of structures. The reflected and transmitted waves are affected by the beginning of the weak interfaces and can be used to detect the presence and/or the location of the weak interfaces.

The incoming wave is considered known and can be represented by

$$u_1 = A\exp i(\omega t - \bar{\xi}x_1) \tag{37}$$

The reflected wave is to be determined and is written as

$$u_1 = B\exp i(\omega t + \bar{\xi}x_1) \tag{38}$$

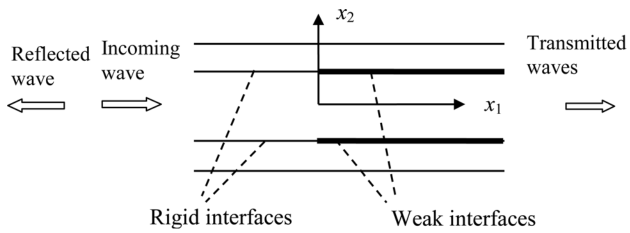

Fig. 3 Joint between two semi-infinite sandwich plates

Equations (37) and (38) both satisfy the equation for a perfectly bonded sandwich plate

$$(h\gamma + 2h'\gamma')u_{1,11} = (h\rho + 2h'\rho')\ddot{u}_1 \tag{39}$$

which implies that

$$(h\gamma + 2h'\gamma')\bar{\xi}^2 = (h\rho + 2h'\rho')\omega^2 \tag{40}$$

There are two transmitted waves given by Eq. (36). At the joint where $x_1 = 0$, we have the following continuity conditions:

$$u_1(0^-) = u_1(0^+)$$
$$u_1(0^-) = u_1'(0^+)$$
$$\mathcal{N}_{11}(0^-) = \mathcal{N}_{11}(0^+) \tag{41}$$

Equation (41) are three equations for determining B, $C^{(1)}$, and $C^{(2)}$. Substitution of Eqs. (36)–(38) into Eq. (41) yields

$$A + B = C^{(1)} + C^{(2)}$$
$$A + B = \beta^{(1)}C^{(1)} + \beta^{(2)}C^{(2)}$$
$$(2h\gamma + 4h'\gamma')\bar{\xi}(B - A) = -\left(2h\gamma + 4h'\gamma'\beta^{(1)}\right)\xi^{(1)}C^{(1)} - \left(2h\gamma + 4h'\gamma'\beta^{(2)}\right)\xi^{(2)}C^{(2)} \tag{42}$$

We are mainly interested in the reflected wave. From Eq. (42), we obtain the reflection coefficient as

$$\frac{B}{A} = \frac{\Delta_1}{\Delta_2} \tag{43}$$

where

$$\Delta_1 = \left(\beta^{(1)} - 1\right)\left[\frac{\left(1 + \alpha\eta\beta^{(2)}\right)X^{(2)}}{(1 + \alpha\eta)\bar{X}} - 1\right] - \left(\beta^{(2)} - 1\right)\left[\frac{\left(1 + \alpha\eta\beta^{(1)}\right)X^{(1)}}{(1 + \alpha\eta)\bar{X}} - 1\right]$$
$$\Delta_2 = -\left(\beta^{(1)} - 1\right)\left[\frac{\left(1 + \alpha\eta\beta^{(2)}\right)X^{(2)}}{(1 + \alpha\eta)\bar{X}} + 1\right] + \left(\beta^{(2)} - 1\right)\left[\frac{\left(1 + \alpha\eta\beta^{(1)}\right)X^{(1)}}{(1 + \alpha\eta)\bar{X}} + 1\right] \tag{44}$$

and

$$\bar{X} = \bar{\xi}h = \Omega\sqrt{\frac{1+\alpha\beta}{1 + \alpha\eta}}, \quad X^{(1)} = \xi^{(1)}h, \quad X^{(2)} = \xi^{(2)}h, \quad \eta = \gamma'/\gamma$$
$$\beta^{(1)} = 1 - \Gamma\left[\Omega^2 - \left(X^{(1)}\right)^2\right], \quad \beta^{(2)} = 1 - \Gamma\left[\Omega^2 - \left(X^{(2)}\right)^2\right] \tag{45}$$

We plot B/A versus Γ for different frequencies in Fig. 4. Consider a specific curve for one frequency first. The overall magnitude of B/A is of the order of 1%. It is small but detectable. For small Γ, B/A is negative which indicates a phase change when the wave gets reflected. For large Γ, B/A is positive. For one particular value of Γ, B/A is zero at which we have total transmission without reflection. In the special case when $\Gamma = 0$, there are no weak interfaces. Therefore, $B/A = 0$ and there are no reflected waves. We are mainly interested in the case of slightly weakened

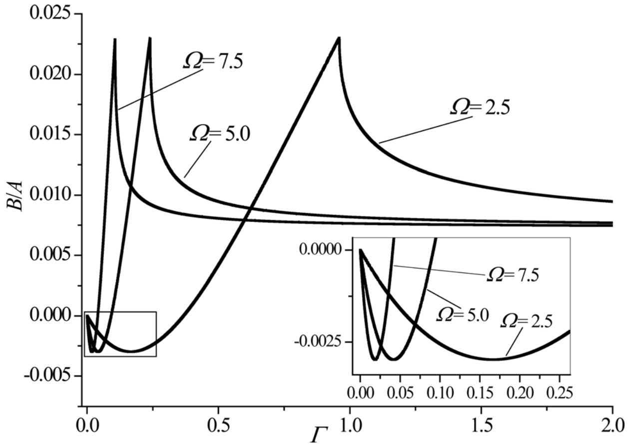

Fig. 4 Reflection coefficient versus Γ ($\alpha = 0.1$, $\beta = 2$, and $\eta = 4.5$)

interfaces with a small Γ. In this case, the magnitude of B/A increases essentially linearly with Γ, ideal for sensing the weakness of the interfaces. For curves with higher frequencies, the linear range becomes narrower.

5 Free Vibration of a Finite Plate

In this section, we consider the free vibration of a finite plate with length $2L$. The two edges are free. From Eqs. (25), (3), and (7), the eigenvalue problem is

$$\begin{aligned} h\gamma u_{1,11} + 2h'\gamma' u'_{1,11} + h\rho\omega^2 u_1 + 2h'\rho'\omega^2 u'_1 = 0, \quad |x_1| < L \\ K' u'_1 = -h\rho\omega^2 u_1 + K' u_1 - h\gamma u_{1,11}, \quad |x_1| < L \\ N_{11} = 2h\gamma u_{1,1} = 0, \quad x_1 = \pm L \\ N'_{11} = 2h'\gamma' u'_{1,1} = 0, \quad x_1 = \pm L \end{aligned} \tag{46}$$

It can be easily verified that the following displacement fields satisfy the edge conditions $(46)_{3,4}$:

$$\begin{aligned} u &= A_n \cos(\zeta_n x_1)\exp(i\omega t) \\ u' &= A'_n \cos(\zeta_n x_1)\exp(i\omega t) \\ \zeta_n &= \frac{n\pi}{L}, \quad n = 0, 1, 2, \ldots \end{aligned} \tag{47}$$

which may be called antisymmetric modes. Similarly, symmetric modes are given by

$$\begin{aligned} u &= B_n \sin(\zeta_n x_1)\exp(i\omega t) \\ u' &= B'_n \sin(\zeta_n x_1)\exp(i\omega t) \\ \zeta_n &= \frac{(2n+1)\pi}{2L}, \quad n = 0, 1, 2, \ldots \end{aligned} \tag{48}$$

Equations (47) and (48) still need to satisfy Eq. $(46)_{1,2}$. In the following, we focus on the symmetric modes in Eq. (48) which, when substituted into Eq. $(46)_{1,2}$, leads to:

$$\begin{aligned} (h\rho\omega^2 - h\gamma\zeta_n^2)B_n + (2h'\rho'\omega^2 - 2h'\gamma'\zeta_n^2)B'_n = 0 \\ \left[1 - \frac{1}{K'}(h\rho\omega^2 - h\gamma\zeta_n^2)\right]B_n - B'_n = 0 \end{aligned} \tag{49}$$

The determinant of the coefficient matrix of Eq. (49) has to vanish. This gives the frequency equation

$$-(h\rho\omega^2 - h\gamma\zeta_n^2) - (2h'\rho'\omega^2 - 2h'\gamma'\zeta_n^2)\left[1 - \frac{1}{K'}(h\rho\omega^2 - h\gamma\zeta_n^2)\right] = 0 \tag{50}$$

or

$$-\left[\Omega^2 - \left(\frac{h}{L}\right)^2 \zeta_n^2\right] - \left[\alpha\beta\Omega^2 - \alpha\eta\left(\frac{h}{L}\right)^2 \zeta_n^2\right]\left\{1 - \Gamma\left[\Omega^2 - \left(\frac{h}{L}\right)^2 \zeta_n^2\right]\right\} = 0 \tag{51}$$

Similar to the two dispersion relations determined by Eq. (32), for each n, Eq. (51) determines two resonant frequencies. One is for the essentially extensional mode with a relatively low frequency; the other is for the essentially thickness-shear mode at a much higher frequency. This is qualitatively different from the extensional vibration of a perfectly bonded sandwich plate which only has the extensional mode.

For finite sandwich plates, the interface shear stress often has concentration near the plate edges which is important for structural strength consideration. With our formulation of the problem, the interface stress under the top film can be conveniently obtained from Eq. (14) as

$$\begin{aligned} T'_{21}|_{-h'} = T_{21}|_h = K'(u'_1 - u_1) = h\rho\ddot{u}_1 - h\gamma u_{1,11} \\ = (h\gamma\zeta_n^2 - h\rho\omega^2)B_n \sin(\zeta_n x_1)\exp(i\omega t) \end{aligned} \tag{52}$$

We introduce a dimensionless shear stress through

$$T_n = \frac{T_{21}h}{\gamma B_n} = \left[\left(\frac{h}{L}\right)^2\left(\frac{2n-1}{2}\pi\right)^2 - \Omega^2\right]\sin\left(\frac{2n-1}{2}\pi\frac{x_1}{L}\right)\exp(i\omega t) \tag{53}$$

For the case of the fundamental mode with $n = 0$, we plot the shear stress distributions corresponding to the essentially extensional and the essentially thickness-shear modes in Figs. 5(*a*) and 5(*b*), respectively. For both cases, the distributions show concentration near the edges. We note that the shear stresses in (*a*) and (*b*) differ by three orders of magnitude and therefore need to be plotted separately. In the essentially extensional mode in Fig. 5(*a*), the core and the films of the sandwich plate move together (in-phase) without much interface shear. In the essentially thickness-shear mode, the core and the films move in opposite directions (out of phase) with significant interface shear and therefore larger shear stress.

Figure 6 shows the effect of the interface shear stiffness on the interface shear stress associated with the essentially thickness-shear mode. Clearly, the stiffness has a strong effect as expected. In the range of Γ shown, the shear stress becomes smaller as Γ increases or when the interface stiffness decreases. Numerical results show that the interface shear stress associated with the essentially extensional mode is insensitive to Γ.

6 Shear-Horizontal Motion

For straight-crested waves propagating in the x_1 direction in a sandwich plate governed by the equations in the present paper, in addition to the extensional waves discussed in the above, there also exist the so-called shear-horizontal or antiplane motions described by $u_3 = u_3(x_1, t)$, $u'_3 = u'_3(x_1, t)$, and $u_1 = u'_1 = 0$. They

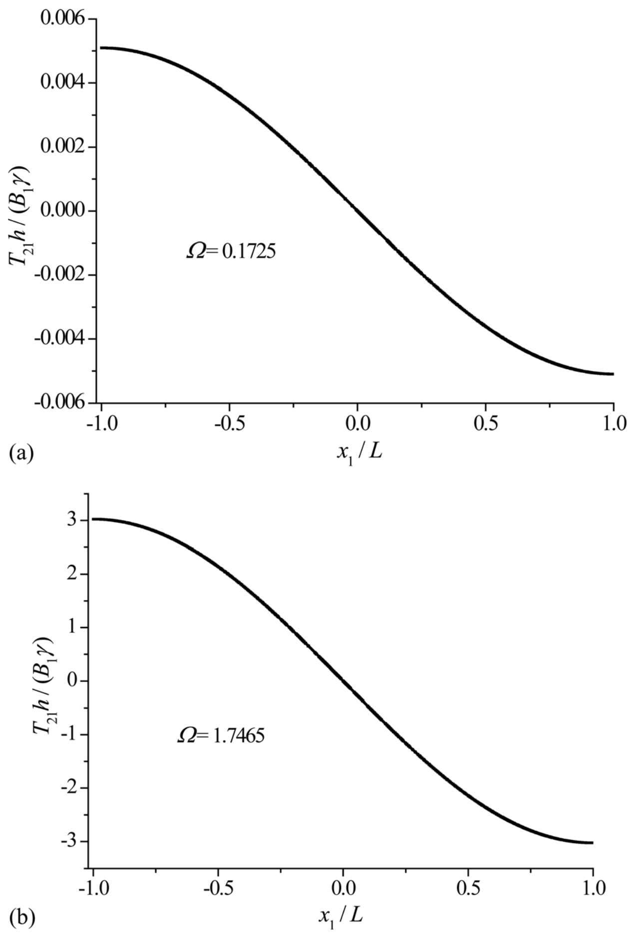

Fig. 5 Shear stress distribution under the upper film ($\Gamma = 2$): (*a*) essentially extensional mode and (*b*) essentially thickness-shear mode

are related to the so-called face-shear and thickness-twist waves in the plate [38]. For these motions, Eqs. (24) and (21) take the following form:

$$
\begin{aligned}
h\gamma_{1331}u_{3,11} + 2h'\gamma'_{1331}u'_{3,11} &= h\rho\ddot{u}_3 + 2h'\rho'\ddot{u}'_3 \\
K'u'_3 &= h\rho\ddot{u}_3 + K'u_3 - h\gamma_{1331}u_{3,11}
\end{aligned}
\tag{54}
$$

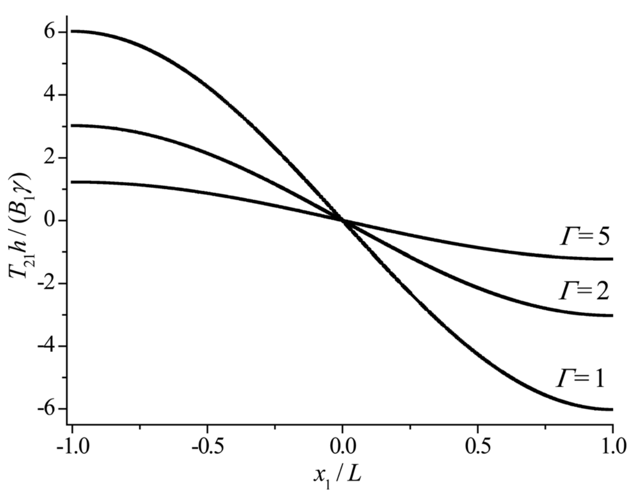

Fig. 6 Effect of interface stiffness on the interface shear stress of the thickness-shear mode

Equation (54) has the same mathematical structure as that of Eq. (25). Therefore, the behaviors of face-shear and thickness-twist waves are expected to be qualitatively similar to those of the extensional and thickness-shear waves discussed in Sec. 3.

7 Conclusion

2D equations for extensional motions of individual layers are combined to form a system of equations for a sandwich plate incorporating the effects of shear-slip interfaces. The equations exhibit a number of behaviors associated with the weak interfaces. For dispersion relations of straight-crested waves in an unbounded plate, in addition to the usual branch for extensional waves, there exists a second branch due to the relative motion among different layers of the plate. At the joint between two semi-infinite plates, one is perfectly bonded and the other has weak interfaces, incoming waves from the perfectly bonded plate are reflected at the joint which can be used to detect the existence and the location of the weak interfaces. For vibrations of finite plates, concentration of the interface shear stress is found near the plate edges. Similar behaviors are predicted for shear-horizontal motions in sandwich plates with weak interfaces.

Acknowledgment

This work was supported by the National Natural Science Foundation of China (Nos. 11272247, 11402187, and 11090333), the National 111 Project of China (No. B06024), and China Postdoctoral Science Foundation funded project (No. 2014M560762). It was also supported by the U.S. Army Research Laboratory/U.S. Army Research Office under Agreement No. W911NF-10-1-0293.

References

[1] Dong, C. X., and Ho, J. C. M., 2013, "Improving Interface Bonding of Double-Skinned CFST Columns," Mag. Concr. Res., **65**(20), pp. 1199–1211.
[2] Marcos-Gomez, D., Ching-Lloyd, J., Elizalde, M. R., Clegg, W. J., and Molina-Aldareguia, J. M., 2010, "Predicting the Thermal Conductivity of Composite Materials With Imperfect Interfaces," Compos. Sci. Technol., **70**(16), pp. 2276–2283.
[3] Massabo, R., and Campi, F., 2014, "An Efficient Approach for Multilayered Beams and Wide Plates With Imperfect Interfaces and Delaminations," Compos. Struct., **116**, pp. 311–324.
[4] Chen, X. F., Ye, J. J., Zhai, Z., and He, Z. J., 2012, "Micromechanical Analysis of Off-Axis Loading of Fiber Reinforced Composites With Imperfect Interface Bonding," Int. J. Mech. Sci., **54**(1), pp. 113–120.
[5] Newmark, N. M., Ceiss, C. P., and Viest, I. M., 1951, "Test and Analysis of Composite Beams With Incomplete Interaction," Proc. Soc. Exp. Stress Anal., **91**, pp. 75–92.
[6] Wu, T.-T., and Chen, Y.-C., 1996, "Dispersion of Laser Generated Surface Waves in an Epoxy-Bonded Layered Medium," Ultrasonics, **34**(8), pp. 793–799.
[7] Lavrentyev, A. I., and Rokhlin, S. I., 1998, "Ultrasonic Spectroscopy of Imperfect Contact Interfaces Between a Layer and Two Solids," J. Acoust. Soc. Am., **103**(2), pp. 657–664.
[8] Jin, F., Kishimoto, K., Inoue, H., and Tateno, T., 2005, "Experimental Investigation on the Interface Properties Evaluation in Piezoelectric Layered Structures by Love Waves Propagation," Key Eng. Mater., **297–300**, pp. 807–812.
[9] Cheng, Z.-Q., Jemah, A. K., and Williams, F. W., 1996, "Theory for Multilayered Anisotropic Plates With Weakened Interfaces," ASME J. Appl. Mech., **63**(4), pp. 1019–1026.
[10] Chen, W. Q., Cai, J. B., Ye, G. R., and Wang, Y. F., 2004, "Exact Three-Dimensional Solutions of Laminated Orthotropic Piezoelectric Rectangular Plates Featuring Interlaminar Bonding Imperfections Modeled by a General Spring Layer," Int. J. Solids Struct., **41**(18–19), pp. 5247–5263.
[11] Handge, U. A., 2002, "Analysis of a Shear-Lag Model With Nonlinear Elastic Stress Transfer for Sequential Cracking of Polymer Coatings," J. Mater. Sci., **37**(22), pp. 4775–4782.
[12] Sedighi, H. M., Shirazi, K. H., and Naderan-Tahan, K., 2013, "Stick-Slip Vibrations of Layered Structures Undergoing Large Deflection and Dry Friction at the Interface," ASME J. Vib. Acoust., **135**(6), p. 061006.
[13] Jones, J. P., and Wittier, J. S., 1964, "Waves at a Flexibly Bonded Interface," ASME J. Appl. Mech., **34**(4), pp. 905–909.
[14] Murtya, G. S., 1975, "A Theoretical Model for the Attenuation and Dispersion of Stoneley Waves at the Loosely Bonded Interface of Elastic Half Spaces," Phys. Earth Planet. Inter., **11**(1), pp. 65–79.
[15] Leungvichcharoen, S., and Wijeyewickrema, A. C., 2003, "Dispersion Effects of Extensional Waves in Prestressed Imperfectly Bonded Incompressible Elastic Layered Composite," Wave Motion, **38**(4), pp. 311–325.

[16] Deng, M. X., Wang, P., and Lv, X. F., 2006, "Study of Second-Harmonic Generation of Lamb Waves Propagating in Layered Planar Structures With Weak Interfaces," IEEE Ultrasonics Symposium, Vancouver, Canada, Oct. 2–6, pp. 1832–1835.

[17] Fan, H., Yang, J. S., and Xu, L. M., 2006, "Piezoelectric Waves Near an Imperfectly Bonded Interface Between Two Half-Spaces," Appl. Phys. Lett., **88**(20), p. 203509.

[18] Bai, Y. Z., Wang, Y. S., and Yu, G. L., 2007, "Subsonic Slip Waves Along the Interface Between Two Piezoelectric Solids in Sliding Contact With Local Separation," Int. J. Eng. Sci., **45**(12), pp. 1017–1029.

[19] Melkumyan, A., and Mai, Y.-W., 2008, "Influence of Imperfect Bonding on Interface Waves Guided by Piezoelectric/Piezomagnetic Composites," Philos. Mag., **88**(23), pp. 2965–2977.

[20] Li, Y.-D., and Lee, K. Y., 2010, "Effect of an Imperfect Interface on the SH Wave Propagating in a Cylindrical Piezoelectric Sensor," Ultrasonics, **50**(4–5), pp. 473–478.

[21] Pang, Y., and Liu, J. X., 2011, "Reflection and Transmission of Plane Waves at an Imperfectly Bonded Interface Between Piezoelectric and Piezomagnetic Media," Eur. J. Mech.-A/Solids, **30**(5), pp. 731–740.

[22] Chen, J. Y., Chen, H. L., and Pan, E., 2008, "Reflection and Transmission Coefficients of Plane Waves in Magnetoelectroelastic Layered Structures," ASME J. Vib. Acoust., **130**(3), p. 031002.

[23] Otero, J. A., Rodríguez-Ramos, R., Bravo-Castillero, J., and Monsivais, G., 2012, "Interfacial Waves Between Two Piezoelectric Half-Spaces With Electro-Mechanical Imperfect Interface," Philos. Mag. Lett., **92**(10), pp. 534–540.

[24] Ferrante, F., and Kipling, A. L., 1994, "Molecular Slip at the Solid-Liquid Interface of an Acoustic-Wave Sensor," J. Appl. Phys., **76**, pp. 3448–3462.

[25] Yang, J. S., Hu, Y. T., Zeng, Y., and Fan, H., 2006, "Thickness-Shear Vibration of Rotated Y-Cut Quartz Plates With Imperfectly Bonded Surface Mass Layers," IEEE Trans. Ultrason., Ferroelectr. Freq. Control, **53**(1), pp. 241–245.

[26] Chen, J. K., Wang, W. C., Wang, J., Yang, Z. T., and Yang, J. S., 2008, "A Thickness Mode Acoustic Wave Sensor for Measuring Interface Stiffness Between Two Elastic Materials," IEEE Trans. Ultrason., Ferroelectr. Freq. Control, **55**(8), pp. 1678–1681.

[27] Zhu, J., Yang, J. S., and Chen, W. Q., 2012, "Locating a Weakened Interface in a Laminated Elastic Plate," Struct. Eng. Mech., **41**(6), pp. 751–758.

[28] Xu, R. Q., and Wu, Y. F., 2008, "Free Vibration and Buckling of Composite Beams With Interlayer Slip by Two-Dimensional Theory," J. Sound Vib., **313**(3–5), pp. 875–890.

[29] Wu, Y. F., Xu, R. Q., and Chen, W. Q., 2007, "Free Vibrations of the Partial-Interaction Composite Members With Axial Force," J. Sound Vib., **299**(4–5), pp. 1074–1093.

[30] Chen, W. Q., Wu, Y. F., and Xu, R. Q., 2007, "State Space Formulation for Composite Beam-Columns With Partial Interaction," Compos. Sci. Technol., **67**(11–12), pp. 2500–2512.

[31] Wang, Y. S., Yu, G. L., Zhang, Z. M., and Feng, Y. D., 2000, "Review on Elastic Waves Propagation Under Complex Interface (Interface Layer) Conditions," Adv. Mech., **30**, pp. 378–389 (in Chinese).

[32] Mindlin, R. D., 1963, "High Frequency Vibrations of Plated, Crystal Plates," *Progress in Applied Mechanics* (The Prager Anniversary Volume), Macmillan, New York, pp. 73–84.

[33] Tsuyoshi, I., Yukiko, I., and Hideaki, N., 2012, "Vibration Analysis of a Self-Excited Vibration in a Rotor System Caused by a Ball Balancer," ASME J. Vib. Acoust., **134**(2), p. 021006.

[34] Tiersten, H. F., Sinha, B. K., and Meeker, T. R., 1981, "Intrinsic Stress in Thin Films Deposited on Anisotropic Substrates and Its Influence on the Natural Frequencies of Piezoelectric Resonators," J. Appl. Phys., **52**(9), pp. 5614–5624.

[35] Tiersten, H. F., 1994, "Equations for the Control of the Flexural Vibrations of Composite Plates by Partially Electroded Piezoelectric Actuators," Proc. SPIE, **2427**, pp. 326–342.

[36] Yang, J. S., 1997, "Equations for the Flexural Motion of Elastic Plates With Partially Electroded Piezoelectric Actuators," Smart Mater. Struct., **6**(4), pp. 485–490.

[37] Liu, N., Yang, J. S., Hu, Y. T., Chen, X. D., and Jiang, W., 2011, "Frequency Shifts in Plate Crystal Resonators Induced by Electric, Magnetic, or Mechanical Fields in Surface Films," IEEE Trans. Ultrason., Ferroelectr. Freq. Control, **58**(12), pp. 2588–2595.

[38] Mindlin, R. D., 2006, *An Introduction to the Mathematical Theory of Vibrations of Elastic Plates*, J. S. Yang, ed., World Scientific, Singapore, pp. 101–154.

[39] Li, P., and Jin, F., 2014, "Effect of an Imperfect Interface in a Quartz Crystal Microbalance for Detecting the Properties of an Additional Porous Layer," J. Appl. Phys., **115**(5), p. 054502.